ELSEVIER

Carbohydrate Research 264 (1994) 1–19

CARBOHYDRATE RESEARCH

Modeling of aldopyranosyl ring puckering with MM3(92)

Michael K. Dowd [a,*], Alfred D. French [a], Peter J. Reilly [b]

[a] *Southern Regional Research Center, U.S. Department of Agriculture, P.O. Box 19687, New Orleans, LA 70179 USA*

[b] *Department of Chemical Engineering, Iowa State University, Ames, IA 50011 USA*

Received 7 April 1994; accepted 10 May 1994

Abstract

The molecular mechanics algorithm MM3 was used to compute energy surfaces for aldopyranosyl rings having a full range of shapes. Energies were plotted against the Φ–Θ puckering coordinates of Cremer and Pople. The $^4C_1$ conformations of the model pyranosyl rings are dominant for both anomers of D-allose, D-galactose, D-glucose, D-mannose, and D-talose, as are the $^4C_1$ conformations of β-D-altropyranose, β-D-gulopyranose, and β-D-idopyranose. α-D-Altropyranose is predicted to exist as an equilibrium of $^1C_4$ and $^4C_1$, α-D-idopyranose as an equilibrium among $^OS_2$, $^1C_4$, and $^4C_1$, and α-D-gulopyranose is predominately $^4C_1$ but has some contribution from $^1C_4$ (18%) and $^OS_2$ (9%). The calculated and measured hydrogen–hydrogen coupling constants agree well, although the energies for the β anomers in water are systematically low by an average of 0.4 kcal/mol. Because the errors in the predicted anomeric ratios are small and are similar for the eight hexoses, and because the only concession to the solvent was a dielectric constant of 3.0, specific solvent effects are apparently small.

Keywords: Molecular modeling; Aldopyranoses; MM3; Molecular mechanics; Conformation; Ring puckering; Allose; Altrose; Galactose; Glucose; Gulose; Idose; Mannose; Talose

1. Introduction

Hexoses exist primarily as pyranosyl and furanosyl rings with pyranosyl forms prevailing in solution and as building blocks for many oligosaccharides and polysaccharides. All experimental evidence indicates that chair forms (Fig. 1) dominate the conformer populations of the 16 aldopyranoses except for a skew form for idose and related derivatives [1,2]. For pyranosyl forms of D-allose, D-galactose, D-glucose, D-mannose, and D-talose, the $^4C_1$

* Corresponding author.

SSDI 0008-6215(94)00185-I

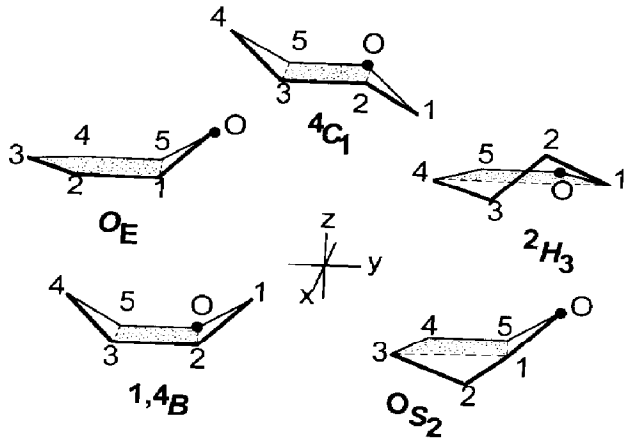

Fig. 1. Representation of aldopyranosyl characteristic conformers: chairs (*C*), boats (*B*), skews (*S*), half-chairs (*H*), and envelopes (*E*).

form is always identified by NMR spectroscopy [3–5] and numerous crystallographic studies. For α-D-altropyranose, an equilibrium of $^4C_1$ and $^1C_4$ is found by NMR spectroscopy [5], while for α-D-idopyranose and related structures the $^OS_2$ is found in addition to the (^2S_O for the L form) two chairs by NMR spectroscopy and computational studies [1,2,6].

Early modeling of aldopyranosyl rings used relatively simple potential functions. In the late sixties, Angyal [7] predicted favored chair conformations and anomer distributions by summing assigned empirical energy values for the axial and equatorial components attached to pyranosyl chairs. Over the next decade, force fields of increasing complexity were applied to the aldopyranoses, generally without structural optimization [8–11]. For glucose, more detailed studies incorporating relaxed rings [12,13] and molecular dynamics [14–16], as well as three studies using semi-empirical quantum techniques [17–19], have appeared. *Ab initio* work on the α- and β-glucopyranosyl $^4C_1$ structures has recently been reported [19,20]. In general, the early studies focused on determining favored ring conformations, while recent work has been directed toward understanding anomeric distribution or the distribution of conformers about the C-5–C-6 bond.

One might surmise that the relative energies of the various ring shapes are well understood. However, our experience and recent published results suggest otherwise. Successful systems for modeling carbohydrates must incorporate treatment of electrostatics and anomeric and exo-anomeric effects. They must also provide a way to deal with the large number of possible conformers that can arise from the variable orientations of the primary and secondary hydroxyl groups. The number of conformers of these molecules rules out *ab initio* quantum mechanics studies with basis sets large enough to be accurate, at least for survey purposes and comparisons of a set of compounds like the aldopyranoses. Questions have been raised about the ability of the semi-empirical quantum technique AM1 to predict energies for these structures [21]. In fact, we have found that AM1 predicts the $^1C_4$ form of β-glucopyranose to be more energetically favorable than $^4C_1$.

The molecular mechanics program, MM3, has been useful for modeling the conformations of disaccharides containing pyranosyl rings [22], although sucrose modeling was less satisfactory [22]. This single discrepancy appears to be related to torsional energy terms associated with the unusual overlapping anomer sequences within sucrose [23]. MM3 and

its precursor, MM2, have also modeled well the ring puckering of fructofuranose [24,25] and arabinofuranose [26]. These results suggest that MM3 could also be successful at predicting the trends and anomalies found among aldopyranosyl isomers.

Joshi and Rao generated the first contoured puckering surfaces for α- and β-D-glucopyranose [12]. These surfaces were based on ring structures with unified substituents and were expressed with the puckering parameters and mapping strategy of Pickett and Strauss [27,28]. More recently, Ragazzi et al. [29] presented a surface puckering plot for an α-L-iduronate derivative based on ring structures optimized with REFINE and with the puckering definition of Cremer and Pople [30,31]. This plot showed that a skew was possible, confirming the NMR results. To our knowledge, no other puckering maps have been presented for aldopyranoses or related derivatives.

Herein, we apply a procedure recently reported for studying ring conformations [32] to aldopyranosyl rings as well as to aldopyranosyl analogues. This method involves controlling atomic positions orthogonal to an initial planar form, in contrast with the obvious method of restraining torsion angles or by the recently proposed procedure of adding puckering constraints to the minimization function [33]. Contoured surfaces are developed on two-dimensional energy grids, similar to those of Pickett and Strauss [27], for the 16 aldohexopyranosyl rings plus cyclohexane, tetrahydropyran, and 2-hydroxytetrahydropyran. Since the 1979 report of Joshi and Rao [12], advances in computing power and software permit the full consideration of the exocyclic rotating group orientations as well as the full optimization of the various ring shapes. In addition, we have used structures corresponding to the local minima to estimate anomeric equilibra and coupling constants, and have correlated these values with available experimental evidence.

2. Computational methods

The 1992 version of MM3 was chosen for this work [34–36]. Differences from the 1990 version that are important for carbohydrate modeling include the addition of an angular dependence to the hydrogen bonding function and an iterative approach to correcting bond lengths associated with anomeric sequences. Median values of the dielectric constant (2.5 to 4.0) best model crystalline glucose [37] and minicomplexes of crystalline disaccharides [22]. In addition, the difference between adiabatic disaccharide ϕ,ψ maps calculated at dielectric constants of 3 and 80 is relatively small, compared to the differences calculated at dielectric constants of 1 and 3. Hence, the dielectric constant was set to 3.0. The energy minimization method was applied with the default termination criterion (1.92 cal/mol). Surfaces were generated from structures optimized by the block-diagonal minimization method, and local minima were isolated using the full-matrix method. Twenty-five to thirty DECstation computers and a VAXstation were used during the study.

Puckered ring structures were generated by orienting a planar pyranosyl ring in the xy plane and systematically moving the C-2, C-4, and O-5 atoms and their substituents in the z direction in 0.1 Å increments from -0.8 Å to $+0.8$ Å, as we have described before [32]. Because of limitations on computer time, it was not practical to consider all 729 (3^6) possible combinations of staggered orientations of the exocyclic hydroxyl and hydroxymethyl groups at each of the 4913 (17^3) puckered ring conformations. Instead we chose

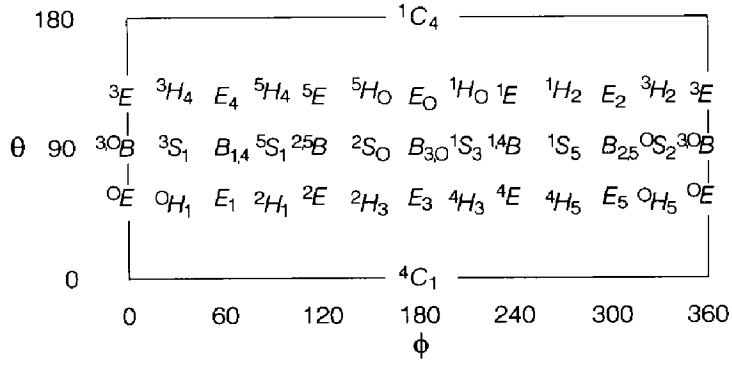

Fig. 2. Locations of characteristic conformers on the surface representing the Cremer–Pople puckering space.

starting conformations by optimizing the 729 combinations of exocyclic orientations for each of the two chair, six boat, six skew, 12 half-chair, and 12 envelope characteristic conformers (Figs. 1 and 2). The lowest energy conformer for each of these forms was used to define a set of preferred staggered exocyclic orientations that were used in the ring puckering calculations. Only 13 to 23 unique sets were needed for each molecule, because some of the combinations of exocyclic orientations were the same for the 38 conformations. For 2-hydroxytetrahydropyran, all three staggered orientations of the hydroxyl group were considered.

Three parameters are needed to describe the puckering of six-atom rings. Within the Cremer–Pople formalism [30,31], these parameters are denoted q, Φ, and Θ. The magnitude of puckering, q, measures the mean deviation of the ring atoms from a plane, while the Φ and Θ parameters reflect the relative orientations of the puckering about the ring. The three parameters could be depicted in a spherical coordinate space. Characteristic conformers are located around a sphere within this space, commonly referred to as a puckering sphere. Ideal chair forms are located at the two poles of this sphere ($\Theta = 0°$ and 180°); ideal boat and skew forms are interspersed around the equator ($\Theta = 90°$); and half-chair and envelope forms are positioned between the poles and equator.

Puckering analysis of pyranose rings is thus a four-dimensional problem in q, Φ, Θ, and energy. In principle, it is possible to generate isoenergy contour surfaces within the puckering spherical coordinate space, although it is difficult to visualize the details of such a graphic. A simpler representation is needed. For ring structures that are not externally constrained, the variations in the magnitude of puckering tend to be small for optimal geometries, regardless of the values of the other two puckering parameters. Hence, the most variable aspects of puckering occur within a shell of the puckering sphere. This shell can be represented as a 2-dimensional rectangular coordinate space in Φ and Θ at optimal values of q, similar to a *plate carrée* projection of the Earth's surface. Isoenergy contour lines can be plotted on this Φ–Θ projection.

These surfaces were generated by dividing the Φ and Θ ranges into $10° \times 10°$ bins. Each of the 4913 Φ, Θ, and q combinations was placed into its appropriate bin, and the lowest energy point from each bin was used to generate points for the map. Only bins containing at least four points per initial structure were considered, eliminating bins that did not have a reasonable range of q values. Of the 648 bins, 524 to 526 were occupied, and generally all of the 13 to 23 starting exocyclic orientations contributed to the final map points. This

procedure results in fairly complete coverage of the Φ–Θ surface, as shown in earlier work (Fig. 7, Ref [32]). A representation of this rectangular space (Fig. 2) shows the positions of the characteristic conformers. Isoenergy contours were generated using SURFER (Golden Software, Golden, CO).

Local minima were found by taking the lowest energy gridpoint structure from each of the low-energy wells on the puckering surface and optimizing it without constraint with the full matrix method, again considering all 729 possible combinations of exocyclic orientations. A conformer assignment (chair, boat, etc.) was made based on the closest characteristic conformer. For minima along the equator, boat, skew, and intermediate skew–boat conformers were assigned by evenly dividing the 360° of Φ between the 24 forms. Our skew–boat labels denote structures along the puckering equator that differ from a "pure" skew or boat by more than 7.5° in Φ. Hydrogen–hydrogen coupling constants were estimated from the populations of local minima with the Karplus equations of Haasnoot et al. [38].

3. Results

Computed Φ–Θ puckering surfaces are shown in Figs. 3 and 4. Fig. 3 gives the surfaces for the three aldopyranosyl analogues contoured at 1 kcal/mol intervals. For all three compounds, local low-energy regions are found near the two poles ($\Theta = 0°, 180°$) and near the equator ($\Theta = 90°$). High-energy ridges corresponding approximately to envelope and half-chair conformers separate the low-energy regions. For the cyclohexane map, six-fold symmetry is apparent around the equator in addition to mirror symmetry through the equator. The map for tetrahydropyran is similar, except that the six-fold symmetry lost by incorporating the oxygen atom into the ring is replaced by a two-fold symmetry along the equator of the map plus the mirror symmetry through the equator. The map for 2-hydroxytetrahydropyran is similar in the general formation of high- and low-energy regions, although the symmetry is lost.

Maps for the 16 aldopyranoses contoured in 2 kcal/mol intervals relative to their global minima are shown in Fig. 4. As found for the analogues, local low-energy regions exist at the poles and at the equator. The equatorial and polar minima are separated by regions of high energy, but the envelope and half-chair forms do not always constitute continuous high-energy ridges between the low-energy regions.

Contours of q over the Φ–Θ region are similar to those given for α-D-psicopyranose [32] and are not shown. The magnitude of puckering changes gradually from ca. 0.55 at the poles (chairs) to 0.75 along the equator (skews and boats). Contour lines of constant q parallel the Φ axis, with local deviations. Plots of q for the three analogues are similar (not shown).

Local minima are denoted on the maps and their puckering values and energies are given in Table 1. For highly symmetric cyclohexane, single chair and skew minima exist, with the former favored by 5.8 kcal/mol. Three minima are found for tetrahydropyran: one chair and two skews ($^1S_3 = {}^3S_1 = {}^OS_2 = {}^2S_O$ and $^1S_5 = {}^5S_1$, numbered as in Fig. 1). The skew minima are within 0.8 kcal/mol of each other but are >5.5 kcal/mol above the chair form. Five local minima are found, two chairs and three skews or intermediate skew–boats, on the 2-hydroxytetrahydropyran map. The two chairs differ by 0.3 kcal/mol, the computed

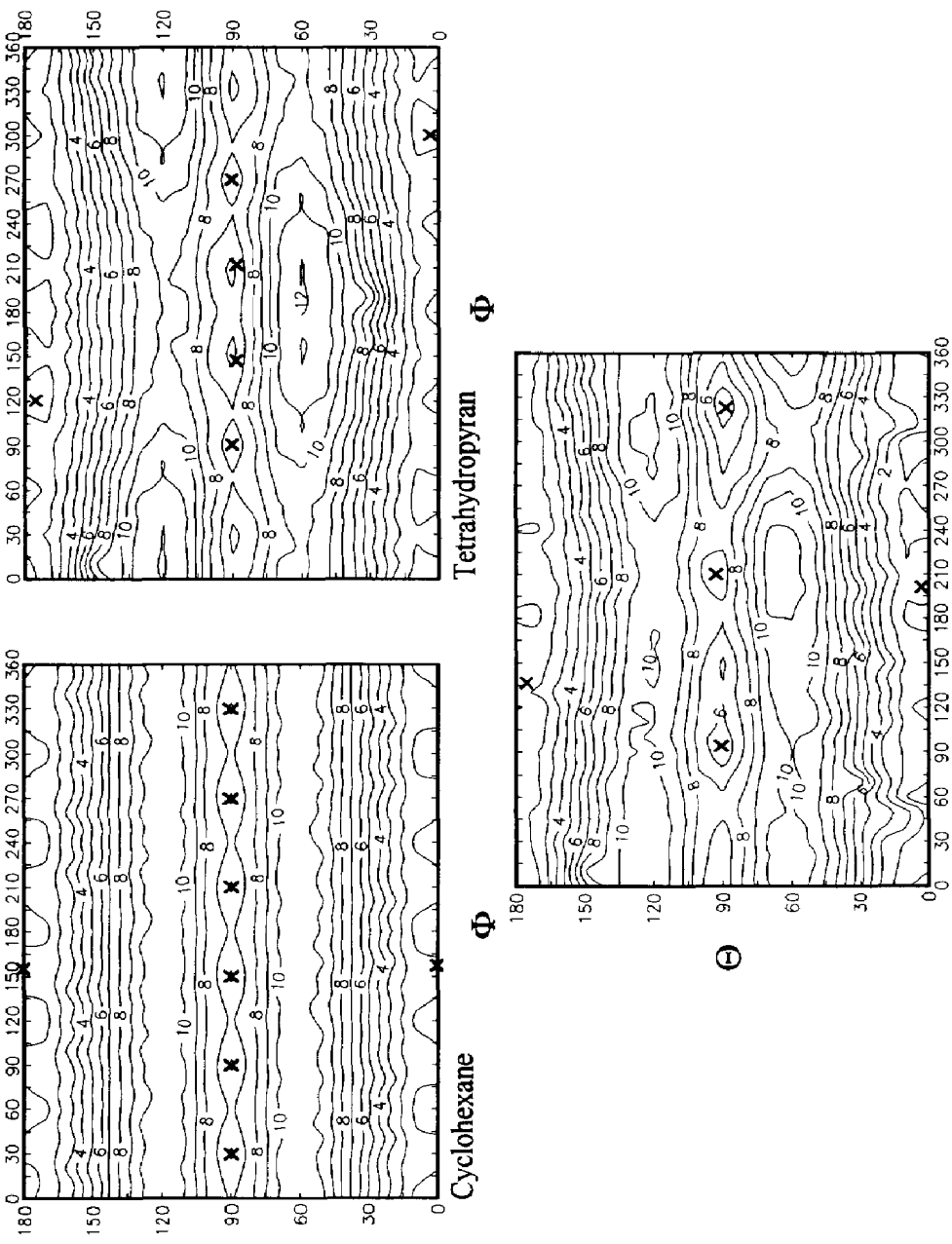

Fig. 3. MM3 Φ–Θ puckering maps for cyclohexane, tetrahydropyran, and 2-hydroxytetrahydropyran. Local minima are denoted with crosses.

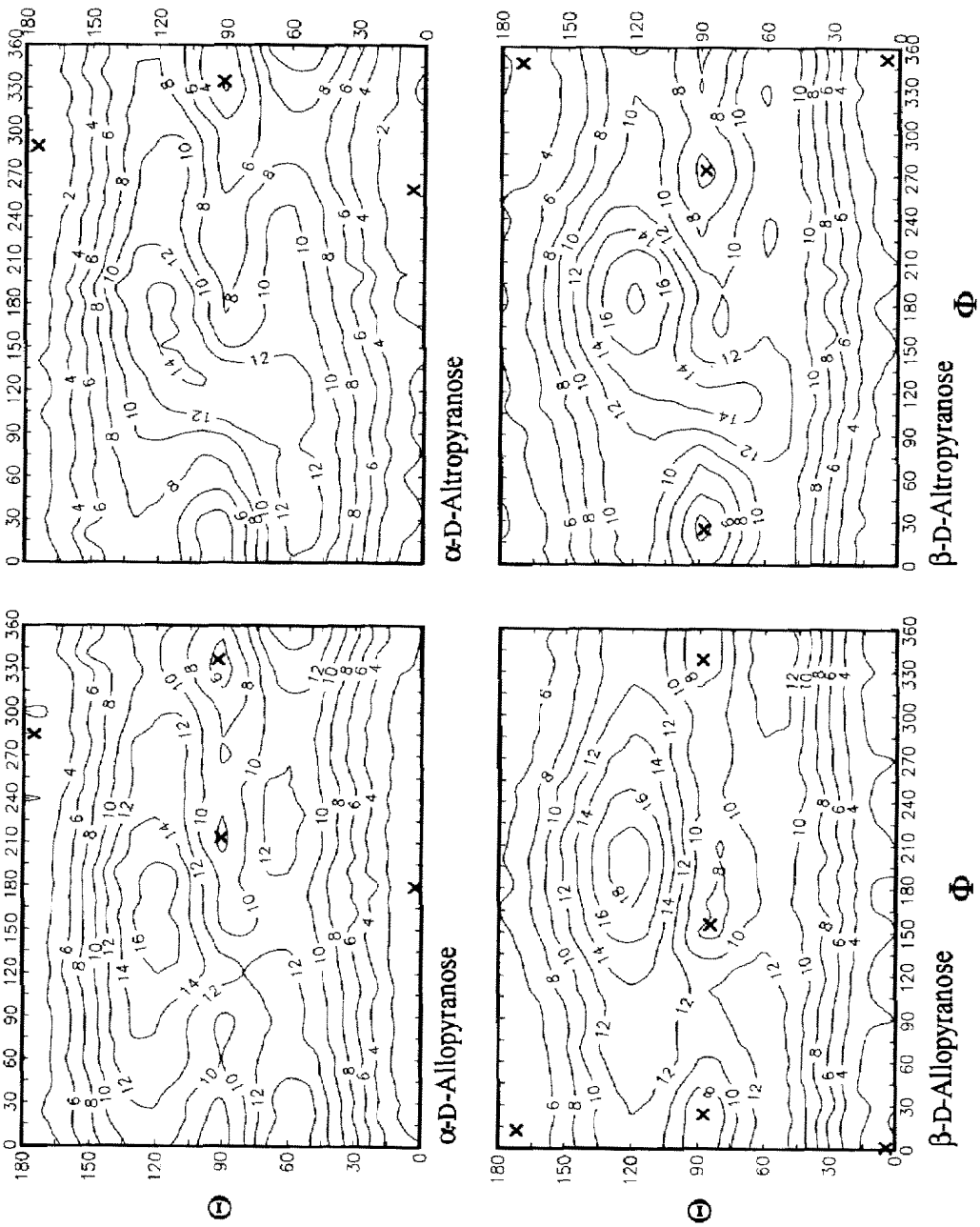

Fig. 4. MM3 Φ–Θ puckering maps for the aldopyranoses. Local minima are denoted with crosses.

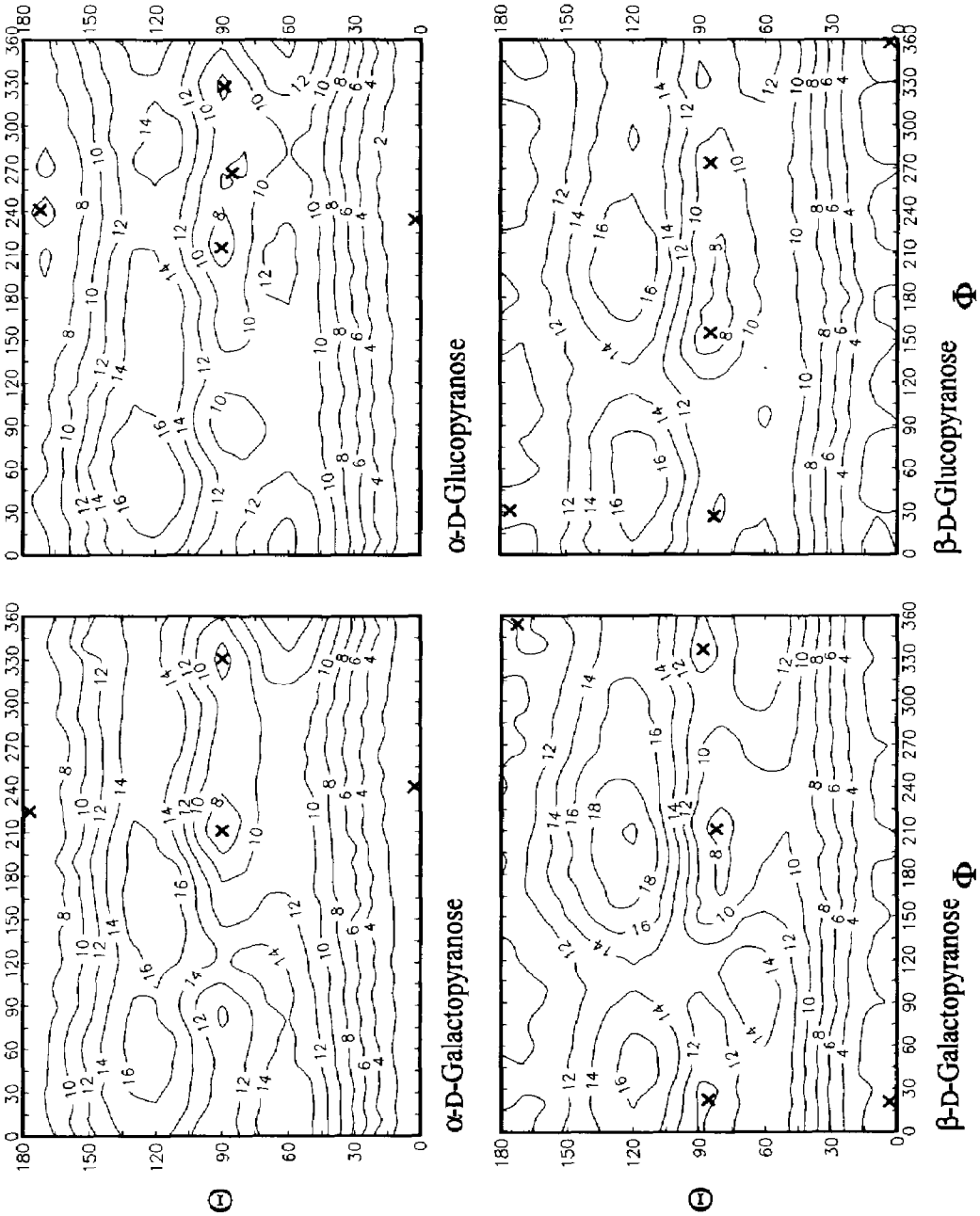

Fig. 4 (continued).

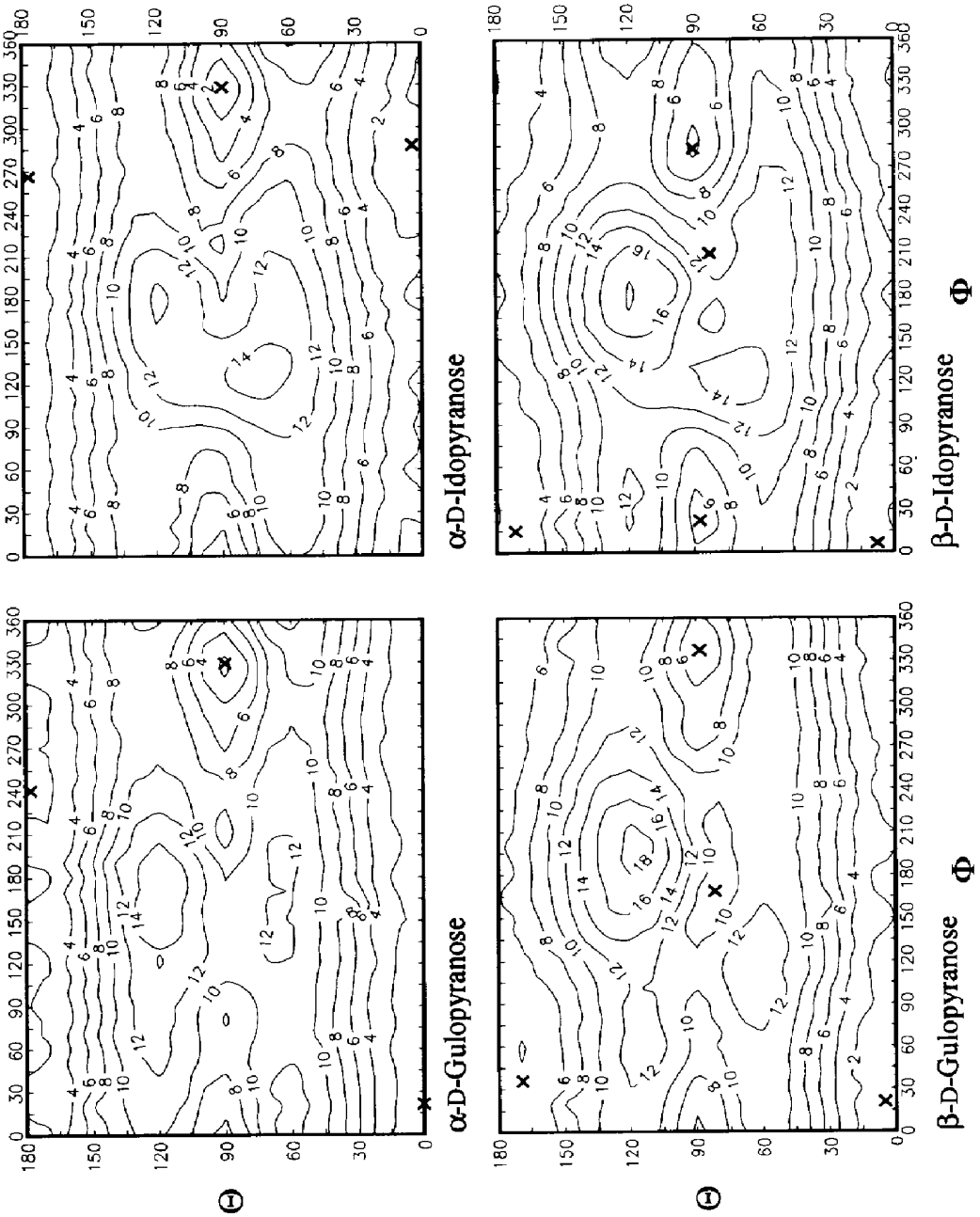

Fig. 4 (continued).

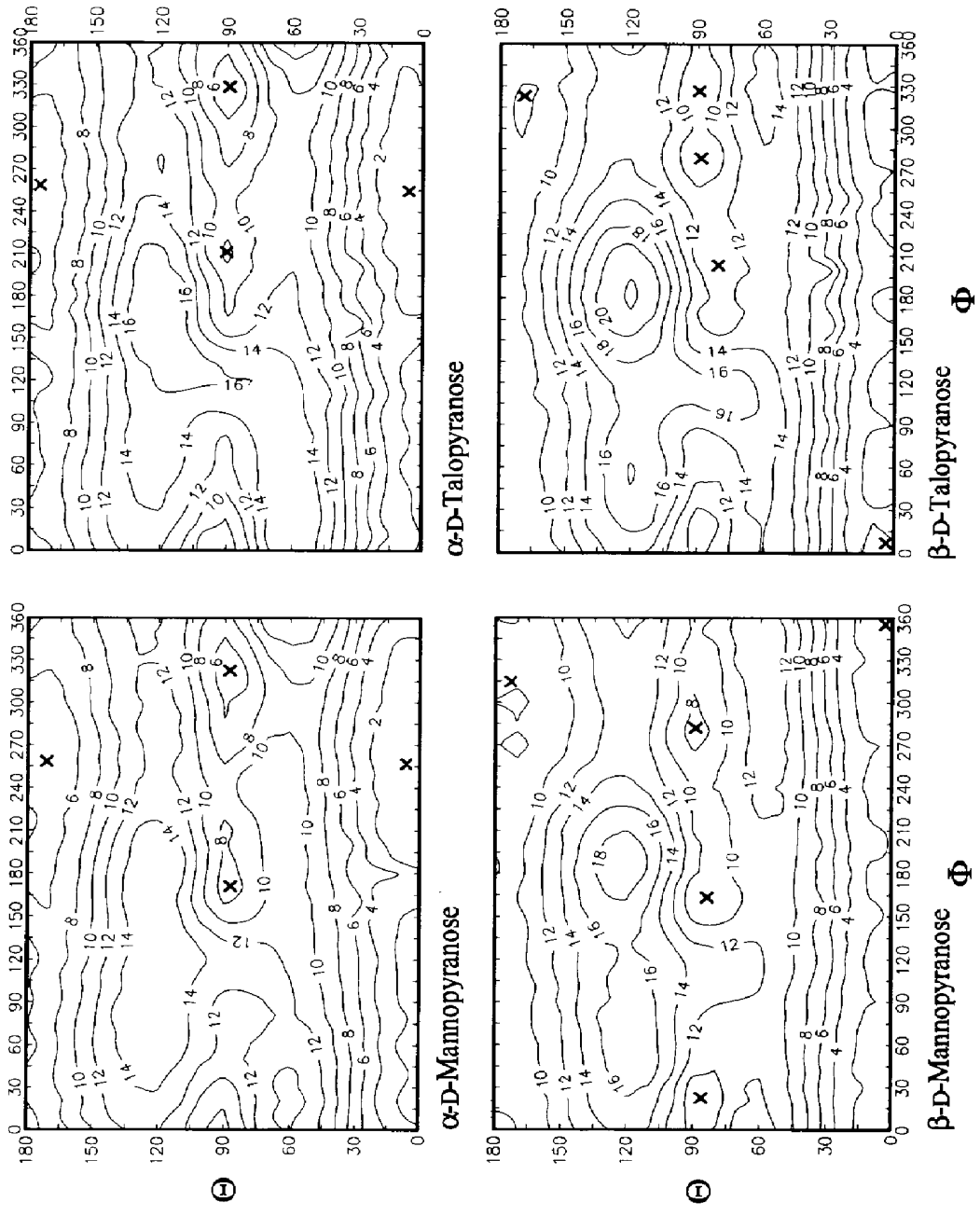

Fig. 4 (continued).

Table 1
Cremer–Pople puckering values and energies for the local minima for the aldopyranoses and analogues from MM3(92) with $\varepsilon = 3.0$

	q (Å)	Φ (degrees)	Θ (degrees)	Approximate characteristic form	Steric energy (kcal/mol)	Relative energy (kcal/mol)
Cyclohexane	0.569	157.6	0.0	C	8.04	0.00
	0.756	150.0	90.0	S	13.80	5.76
Tetrahydropyran	0.573	300.0	3.8	C	8.46	0.00
	0.755	147.5	88.4	$^{1}S_{3}$	13.92	5.54
	0.749	270.0	90.0	$^{1}S_{5}$	14.66	6.20
2-Hydroxytetrahydropyran	0.552	201.4	3.2	$^{4}C_{b}^{1}$	7.47	0.00
	0.582	136.8	175.5	$^{1}C^{4}$	7.80	0.33
	0.729	322.9	88.6	$^{O}S_{2}$	11.44	2.97
	0.756	94.3	90.6	$^{5}S_{1}$	12.42	3.95
	0.768	210.2	92.8	$^{1}S_{3}$	14.66	6.19
α-D-Allopyranose	0.560	179.4	2.6	$^{4}C_{1}$	13.09	0.00
	0.547	284.8	175.3	$^{1}C_{4}$	14.50	1.41
	0.760	336.4	92.4	$^{O}S_{2}$	17.56	4.47
	0.762	213.6	90.3	$^{1}S_{3}$	20.22	7.13
β-D-Allopyranose	0.590	1.4	4.1	$^{4}C_{1}$	11.65	0.00
	0.501	12.3	171.8	$^{1}C_{4}$	15.56	3.91
	0.766	24.0	87.2	$^{3}S_{1}$	17.34	5.69
	0.760	338.8	88.1	$^{O}S_{2}/^{3,O}B$	17.74	6.09
	0.702	155.6	84.4	$^{2}S_{O}$	18.56	6.91
α-D-Altropyranose	0.552	289.6	174.8	$^{1}C_{4}$	13.28	0.00
	0.539	259.7	5.2	$^{4}C_{1}$	13.64	0.36
	0.772	334.6	90.8	$^{O}S_{2}$	14.78	1.50
β-D-Altropyranose	0.574	351.3	5.7	$^{4}C_{1}$	12.55	0.00
	0.519	348.6	170.5	$^{1}C_{4}$	15.02	2.47
	0.773	24.7	87.5	$^{3}S_{1}$	15.44	2.89
	0.754	274.3	87.5	$^{1}S_{5}$	17.53	4.98
α-D-Galactopyranose	0.554	242.0	2.7	$^{4}C_{1}$	11.30	0.00
	0.538	225.2	177.0	$^{1}C_{4}$	16.95	5.65
	0.761	211.8	90.1	$^{1}S_{3}$	17.11	5.81
	0.744	331.0	90.0	$^{O}S_{2}$	18.24	6.94
β-D-Galactopyranose	0.586	21.5	3.7	$^{4}C_{1}$	10.40	0.00
	0.693	211.4	82.2	$^{1}S_{3}$	17.20	6.80
	0.752	336.7	88.2	$^{O}S_{2}$	19.01	8.66
	0.758	23.0	85.8	$^{3}S_{1}$	19.16	8.76
	0.497	354.0	172.5	$^{1}C_{4}$	19.24	8.84
α-D-Glucopyranose	0.565	234.4	2.7	$^{4}C_{1}$	10.75	0.00
	0.525	241.6	172.1	$^{1}C_{4}$	15.95	5.20
	0.774	215.0	90.3	$^{1}S_{3}$	17.26	6.51
	0.750	267.3	85.6	$^{1}S_{5}$	18.00	7.25
	0.739	328.0	89.0	$^{O}S_{2}$	18.08	7.33
β-D-Glucopyranose	0.598	358.0	3.7	$^{4}C_{1}$	9.76	0.00
	0.715	155.1	84.6	$^{2}S_{O}$	16.27	6.51
	0.472	31.3	175.6	$^{1}C_{4}$	18.34	8.58
	0.723	274.0	84.6	$^{1}S_{5}$	18.42	8.66
	0.730	27.2	82.9	$^{3}S_{1}$	18.94	9.18

Table 1 (continued)

	q (Å)	Φ (degrees)	Θ (degrees)	Approximate characteristic form	Steric energy (kcal/mol)	Relative energy (kcal/mol)
α-D-Gulopyranose	0.548	21.6	0.2	$^4C_1$	14.01	0.00
	0.556	240.8	177.8	$^1C_4$	14.85	0.84
	0.752	329.3	89.8	$^OS_2$	15.26	1.25
β-D-Gulopyranose	0.576	20.9	5.1	$^4C_1$	12.01	0.00
	0.520	35.7	169.2	$^1C_4$	15.61	3.60
	0.767	337.0	88.2	$^OS_2$	15.69	3.68
	0.655	168.8	81.7	$^2S_O/B_{3,O}$	20.44	8.43
α-D-Idopyranose	0.777	328.6	89.8	$^OS_2$	13.06	0.00
	0.569	266.8	177.4	$^1C_4$	13.24	0.18
	0.531	287.8	4.3	$^4C_1$	13.61	0.55
β-D-Idopyranose	0.568	6.2	7.9	$^4C_1$	12.62	0.00
	0.536	15.2	171.4	$^1C_4$	14.87	2.25
	0.738	282.9	90.2	$^1S_5/B_{2,5}$	15.72	3.10
	0.785	22.6	87.6	$^3S_1$	17.16	4.50
	0.664	209.7	83.0	$^1S_3$	22.74	10.12
α-D-Mannopyranose	0.550	257.1	6.2	$^4C_1$	11.18	0.00
	0.761	322.6	87.9	$^OS_2$	15.42	4.24
	0.537	258.5	171.0	$^1C_4$	15.56	4.38
	0.714	171.4	87.1	$^2S_O/B_{3,O}$	17.99	6.81
β-D-Mannopyranose	0.582	355.6	3.6	$^4C_1$	11.28	0.00
	0.760	282.3	89.2	$^1S_5/B_{2,5}$	18.14	6.86
	0.491	314.5	173.0	$^1C_4$	18.42	7.16
	0.686	163.8	83.8	$^2S_O/B_{3,O}$	18.79	7.51
	0.752	22.6	86.0	$^3S_1$	19.21	7.91
α-D-Talopyranose	0.550	254.8	6.4	$^4C_1$	11.79	0.00
	0.768	328.6	89.1	$^OS_2$	15.48	3.69
	0.552	258.6	175.3	$^1C_4$	16.32	4.52
	0.758	211.3	90.2	$^1S_3$	19.04	7.25
β-D-Talopyranose	0.584	7.1	3.8	$^4C_1$	11.59	0.00
	0.523	323.2	168.9	$^1C_4$	18.96	7.37
	0.764	326.9	89.5	$^OS_2$	19.54	7.95
	0.729	279.0	88.6	$^1S_5/B_{2,5}$	19.67	8.08
	0.686	203.5	80.5	$^1S_3$	21.48	9.89

[a] Corresponds to axial form.
[b] Corresponds to equatorial form.

energy difference for the conversion of the axial and equatorial orientations of the anomeric hydroxyl group. The next lowest energy minimum corresponds to a skew, 3 kcal/mol above the global minimum. The lower relative energy of the skew form of 2-hydroxytetrahydropyran (compared to the relative energy of the skew form of tetrahydropyran) indicates that there is a 2 kcal/mol stabilization of the skew form because of the addition of the anomeric hydroxyl group.

Three to seven minima are found for each aldopyranose (Table 1), including both chairs plus at least a single skew. Occasionally, a skew–boat minimum was found, generally with high relative energy. Boat forms did not correspond to minima.

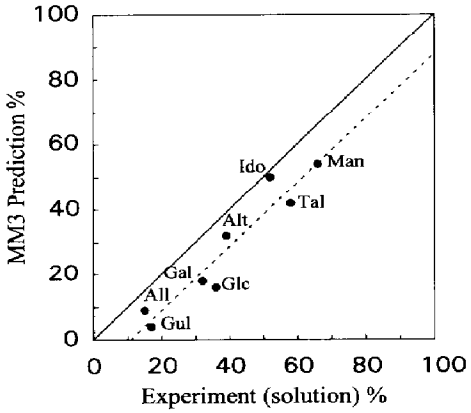

Fig. 5. Percentage of the α-anomeric form of aldopyranoses by MM3 steric energies ($\varepsilon = 3.0$) versus the experimental results in water as tabulated by Angyal [39,40]. The dashed line represents a least-squares linear fit of the modeled percentage of the α form. The solid line indicates perfect agreement.

Based on MM3 steric energies, the pyranosyl forms of β-D-allose, β-D-altrose, α- and β-D-galactose, α- and β-D-glucose, β-D-gulose, β-D-idose, α- and β-D-mannose, and α- and β-D-talose, all favor $^4C_1$ ($>97.5\%$), as does α-D-allose ($>91\%$). The α-altropyranosyl model has an equilibrium between $^1C_4$ (61%) and $^4C_1$ (33%), and the α-gulopyranosyl model is predominately $^4C_1$ (73%), but is also present as $^1C_4$ (17.5%) and as $^OS_2$ (9.5%). The α-idopyranosyl model includes $^OS_2$ (47%), $^1C_4$ (35%), and $^4C_1$ (18%) conformers.

For aldopyranosyl $^4C_1$ conformers, q varies from 0.519 to 0.598. For those $^1C_4$ structures that are energetically unfavorable (with mostly or all axial substituents), the expected van der Waals repulsion of the axial hydroxyl and hydroxymethyl groups produces stress within the ring. The effects are most pronounced for β-glucopyranose. For this sugar, the ring is relatively flattened ($q = 0.472$) and the C-5–O-5–C-1 intraring oxygen valence angle exceeds 120° compared to the corresponding $^4C_1$ values of 0.598 and 113°. Such effects are less dramatic but still apparent for galactose and mannose, and lessen further as the $^1C_4$ becomes more energetically favorable (with more equatorial groups).

A plot of the calculated versus experimental aqueous α-anomeric ratios is shown in Fig. 5. While the agreement is good, there appears to be a systematic overprediction of the β form by up to 20 percentage points compared to experimental aqueous results. This was also observed for the MM3 estimated anomeric ratios of psicopyranose and psicofuranose [32] as well as for the disaccharides gentiobiose and isomaltose [41] (although the exocyclic orientations for these latter molecules were not exhaustively searched).

Calculated hydrogen–hydrogen coupling constants are given in Table 2 together with experimental results. They are generally in good agreement with the root-mean-square (rms) difference between modeled and measured $^3J_{H,H}$ coupling constants being 0.77 Hz.

4. Discussion

Brant and co-workers [11] and Joshi and Rao [12] both studied alternate ring forms for glucopyranose. The first workers had the $^1C_4$ and several skew and boat energies substantially higher than the MM3 or the Joshi and Rao models. The Joshi and Rao puckering

Table 2
Comparison of modeled and experimental hydrogen–hydrogen coupling constants

Pyranose	$^3J_{1,2}$ (Hz)	$^3J_{2,3}$ (Hz)	$^3J_{3,4}$ (Hz)	$^3J_{4,5}$ (Hz)	Ref
α-Allose	3.1	2.5	2.8	8.7	This work
	4.0				5
β-Allose	7.2	3.0	2.8	9.4	This work
	8.1				5
	8.5	3.3	3.2	9.5	54
α-Altrose	5.3	7.3	3.0	4.3	This work
	3.0				5
β-Altrose	1.4	3.5	3.1	9.2	This work
	1.3				5
α-Galactose	3.6	9.0	2.9	0.6	This work
	~3				5
	3.8	10.0	3.8	1.0	54
β-Galactose	7.1	9.0	3.0	0.6	This work
	7.2				5
	8.0	10.0	3.8	1.0	54
α-Glucose	3.4	9.0	8.7	9.4	This work
	3.5				5
	3.6	9.5	9.5	9.5	54
β-Glucose	7.2	8.9	8.6	9.4	This work
	7.5				5
	7.8	9.5	9.5	9.5	54
α-Gulose	3.1	2.9	4.5	1.9	This work
	~4				5
β-Gulose	7.2	3.1	3.4	0.6	This work
	8.5				5
	8.3	3.6	3.6	0.8	54
α-Idose	5.1	8.3	5.9	3.6	This work
	5.6				5
	6.0	8.1	7.9	5.0	1
β-Idose	1.3	3.5	3.1	0.8	This work
	1.6				5
	1.6	3.8	3.7	1.8	1
α-Mannose	2.3	3.1	8.8	9.4	This work
	1.4				5
	1.8	3.8	10.0	9.8	1
β-Mannose	1.2	3.0	8.6	9.4	This work
	1.0				5
	1.5	3.8	10.0	9.8	54
α-Talose	2.3	2.9	2.5	0.4	This work
	1.7				5
	1.9	3.2	3.2	1.3	53
β-Talose	1.3	2.7	2.8	0.6	This work
	1.2				5
	1.2	3.2	3.2	1.2	53

surfaces are similar to those reported here, differing most in the energies (1.5 to 4.0 kcal/mol) of the $^1C_4$ and skew structures. Changing ε from 3.0 to 1.0 made the MM3 value for the $^1C_4$ of β-glucopyranose comparable to their result.

Many crystal structures that contain aldopyranosyl moieties have been reported. All have been found as $^4C_1$ with Θ values that typically range from 4° to 8°, comparable to the modeled values. The largest Θ reported for a glucopyranosyl moiety has been 13° for the central ring of the trisaccharide panose [42], corresponding to ~2 kcal/mol in internal energy above the MM3 global minimum. On the Joshi and Rao surface [12] the same Θ corresponds to ~3 kcal/mol, indicating that their surface is somewhat steeper than the MM3 surface, although differences in puckering definitions may account for this discrepancy. As crystal lattice energies of ca. 30 to 45 kcal/mol/residue are typical for monosaccharides and small oligosaccharides [22,43], 2 kcal/mol of excess internal energy could readily be accommodated within the crystal matrix. Based on modeling results for panose, it does not appear that an intramolecular hydrogen bond connecting the first and third moieties stabilizes the large Θ value (work in progress).

Our maps contain irregularities that result from the increment size used to move atoms, from the type of plot projection used, and to a lesser degree, from the limited number of exocyclic orientations considered. The plots lose some definition because the limited sets of conformers forming a discrete set of q are binned across the Φ–Θ surfaces. Their quality could be improved by using a finer grid to generate the puckered structures, an approach that would require more computer time. For example, a 0.05 Å interval in the z-coordinate direction covering the same puckering region would yield a 35 937 (33^3) point puckering grid compared to the 0.1 Å interval, which yields a 4913 (17^3) point grid. In addition, exhaustive searching of favorable exocyclic orientations has not been conducted over the entire map surface but only for the 38 characteristic conformers. While this does cover the regions containing important minima (chairs, skews, and boats) and potential maxima that might correspond to barriers on intraconversion paths between low-energy regions (half-chairs and envelopes), it would not include other transition regions, e.g., the intraconversion of skews and boats. Finally, distortion of the surface occurs because of the problems in representing a spherical coordinate system on a rectangular surface. While several projections are used in cartography, none eliminate the problem. Hence, we have chosen to use the simple *plate carrée* projection also used by Pickett and Strauss [27]. In this representation, the energy surface is increasingly stretched when moving from the equator toward either pole, and as a consequence a reduced number of points are used in representing the space as Θ approaches 0° or 180°. Hence, contouring becomes less accurate near the poles. In principle, the poles represent a single point on the puckering sphere, yet in some cases contour lines intersect the $\Theta = 0°$ and 180° axes, a manifestation of this problem.

Bearing in mind the above approximations used in generating these maps, the surfaces in fact do reasonably represent the puckering space. Essentially all of the local minima lie within distinct low-energy wells, and the high-energy regions correspond to characteristic conformers that could be thought of as transition structures between stable forms. Experimental results, where available, are consistent with the general topology of these surfaces. For cyclohexane, the experimental value of ΔH for the chair to skew transformation is 5.5 kcal/mol [44] with a transition barrier, $\Delta H^{\ddagger}$, of 10.8 kcal/mol. [45] These numbers agree with the MM3 results of 5.8 and ~10.5 kcal/mol, respectively, as well as with the force-field calculations of Hendrickson [46] and Pickett and Strauss [27] and the recent *ab initio* studies of Dixon and Komornicki [47] and Ferguson et al. [48]. Tetrahydropyran has a chair-to-skew transition barrier of 10.1 (±1.2) [49] to 11.6 (±1.9) [50] kcal/mol, in

reasonable agreement with the MM3 value of ~9.4 kcal/mol. For 2-hydroxytetrahydropyran, the calculation favors the axial form by 0.33 kcal/mol. This contrasts with the experimental value determined in a fluorotrichloromethane–trichloromethane-*d* mixture at relatively low temperatures, which favors the equatorial form by 0.63 kcal/mol (ΔH) [51]. This relatively large difference is difficult to rationalize, although it has been noted that there is potential for intermolecular hydrogen bonding for this compound that may effectively stabilize the equatorial form in the experimental study [51]. Recent 6-31G* single-point *ab initio* calculations on structures optimized at the 3-21G level also favor the axial form by 1.2 kcal/mol [52].

Our procedure for finding minima implicitly assumes that all exocyclic orientations are populated to some degree. If at a given ring puckering, any of the 729 exocyclic starting structures optimized to a lower energy minimum region of the puckering space, the initial region was not assumed to correspond to a minimum. The main effect of this was to reduce the number of indicated minima along the Φ–Θ equator to a few. For example, the apparent minimum in the low-energy region near $\Phi = 90°$ of α-D-galactopyranose [surrounded by an unlabeled 10 kcal/mol contour (Fig. 4)] migrated to the minimum near $\Phi = 330°$ after optimizing all possible exocyclic structures. Occasionally, optimizing a local low-energy structure along the equator ($\Theta = 90°$) yielded a chair form. For example, the $\Phi = 90°$ region of α-D-glucopyranose has a pathway via the exocyclic orientational variations that leads to the $^4C_1$. From this we conclude that not all skew and boat regions are separated from chairs by even higher energy half-chair or envelope forms.

Because pyranoses are hemiacetals, both mutarotation and pseudorotation are conceivable mechanisms for conversion of conformations. The high-energy hills (7 to 9 kcal/mol for α-D-idopyranose and α-D-altropyranose) between the poles and equator suggest that pseudorotation between chair forms is a relatively slow process. Calculated rate constants for chair to skew–boat conversion for cyclohexane and tetrahydropyran were given by Pickett and Strauss [27] as $3.8 \times 10^3\ s^{-1}$ and $2.2 \times 10^4\ s^{-1}$, respectively, at 300 K. Serianni et al. [1,53] reported ring-conversion rate constants (related to rate constants for ring opening and closing) between anomeric five- and six-atom ring forms on the order of 10^4 to $10^5\ s^{-1}$ at 337 K. After accounting for the temperature difference, these rate constants are of the same order of magnitude. Thus, pseudorotation may be an important mechanism for intraconversion between energetically favored ring forms.

NMR hydrogen coupling between H-1 and H-2 yielded the first quantitative description of aldopyranosyl ring puckering [3–5]. More recently, other ^{1}H NMR peaks have been assigned and additional coupling constants reported [1,53,54]. In general, the agreement between the values calculated from our modeling and the measured results is good, although some deviations are seen where an equilibrium between ring forms is evident. The rms deviation between the model and reported experimental values of $^3J_{H,H}$ is 0.77, compared with an inherent uncertainty in the model of Haasnoot et al. [38] of ca. 0.4. The largest deviation ($\Delta^3J_{1,2} = 2.3$) is found for α-D-altropyranose, which exists as an equilibrium between the chair forms, for which the Haasnoot method yields values of $^3J_{1,2}(^4C_1) = 2.2$ and $^3J_{1,2}(^1C_4) = 7.0$. Thus, the experimental value is very sensitive to the equilibrium of these two forms. The MM3 model suggests that the $^1C_4$ is preferred (68%) whereas the experimental result indicates that the $^4C_1$ is preferred (70%).

The calculations for α-D-gulopyranose suggest a small presence of the $^1C_4$ (18%) and $^OS_2$ (9%) in addition to the $^4C_1$. Unfortunately, experimental confirmation of these additional forms may be difficult, as the α anomer is present to only a small degree in equilibrium with the β form, and because the *syn* orientations of the H-1 and H-2 atoms in both chairs and the skew yield $^3J_{1,2}$ coupling constants that are all similar ($^3J_{1,2}(^4C_1) = 3.4$, $^3J_{1,2}(^1C_4) = 1.4$, $^3J_{1,2}(^OS_2) = 3.5$). The $^3J_{3,4}$ and $^3J_{4,5}$ coupling constants might be useful in this regard as there is a larger difference between the two chair forms [$^3J_{3,4}(^4C_1) = 3.5$ and $^3J_{3,4}(^1C_4) = 8.5$; $^3J_{4,5}(^4C_1) = 0.7$ and $^3J_{4,5}(^1C_4) = 5.9$], although these peaks will be more difficult to assign within the spectrum.

Unlike the early results of Sundararajan and Rao [8], MM3 has reproduced Reeves' Δ2 effect [55], where an up C-2 hydroxyl orientation (i.e., axial for the $^4C_1$) destabilizes the β-anomeric form. For each pair of otherwise identical pyranosyl rings, a down orientation of the C-2 hydroxyl (i.e., equatorial for the $^4C_1$) has a higher concentration of the β-anomeric form. Stoddard [56] later commented that because the anomeric ratio of 2-deoxy-D-*arabino*-hexopyranose ($\alpha = 47\%$) [57] was between that of glucopyranose ($\alpha = 36\%$) and mannopyranose ($\alpha = 66\%$), there must also be a stabilizing effect of an equatorial C-2 hydroxyl on the β-anomeric form. Similar differences are found for the C-2 epimers galactopyranose ($\alpha = 32\%$) and talopyranose ($\alpha = 58\%$) plus the 2-deoxy-D-*lyxo*-hexopyranose ($\alpha = 51\%$) [57]. The other two epimer pairs show the same effect, but the analysis is complicated somewhat by the presence of multiple conformers for the α-anomeric forms. A $^1C_4$ α anomer with an up C-2 hydroxyl is conformationally equivalent to a $^4C_1$ β anomer with a down C-2 hydroxyl through the O-5 to C-2 part of the molecule. Therefore, the same stabilizing influence of a down C-2 hydroxyl on the β forms of the $^4C_1$ may also be helping to stabilize the $^1C_4$ of the corresponding α anomers with up C-2 hydroxyls, i.e., altose and idose. Within the MM3 formalism, the energy differences appear to be associated with torsion angle and dipole–dipole contributions.

The comparison of experimental aqueous and calculated anomeric ratios shown in Fig. 5 indicates that MM3 modeling is able to predict trends in the anomeric distribution. However, MM3 systematically overpredicts the β form by up to 20 percentage points. The discrepancies appear to be represented by systematic and random components. By calculating the energy difference required to correct the MM3 modeled predictions, we estimate a mean energy correction equal to 0.41 ± 0.26 kcal/mol. Although the literature is less complete, anomeric distributions have been studied in less polar solvents, in particular pyridine ($\varepsilon = 12.4$). In this solvent, the α-aldopyranosyl anomer appears to be more prevalent than in water, possibly due to the existence of a solvent effect on the anomeric ratio that has recently been debated by several authors [15,16,19]. The mean energy correction needed to correct the MM3 anomeric ratios when compared with experimental work in pyridine is 0.69 ± 0.31 kcal/mol. While these errors are of the order of accuracy of "state-of-the-art" molecular mechanics programs, entropic factors as well as solvation cannot be totally discounted and may contribute to the deviations. Yet it is apparent that much of the anomeric behavior is accounted for by energetic components included within the MM3 force field. Therefore, unless a large, conformationally dependent entropy offsets a large solvation energy for each anomeric pair studied, we conclude that these effects are less significant. Our results support the opinion that there is a relatively small solvent effect and agree qualitatively with the conclusions of Cramer and Truhlar [19]. Our energy corrections

of ca. 0.7 kcal/mol in pyridine and 0.4 kcal/mol in water indicate that the 0.3 kcal/mol difference represents an estimate of the solvent effect on the anomeric ratio.

5. Conclusions

New studies on pyranosyl rings were needed because of the limited nature of previous studies and because other computational and experimental techniques have raised questions that warrant in-depth investigations of ring structure. We found MM3 to model well the puckering in aldopyranose rings. In general, $^4C_1$ forms are favored, although equilibra among two- and three-ring forms are predicted for α-D-altropyranose and α-D-idopyranose, respectively, as has been suggested from NMR studies. α-D-Gulopyranose may also exist as $^1C_4$ and as $^OS_2$, although the populations of these conformers are smaller than the same forms of D-altrose and D-idose. Modeled NMR hydrogen–hydrogen coupling constants about the pyranosyl ring also agree well with experimental results. The equilibra between anomers for all of the sugars are also reproduced. The small difference between experimental aqueous values and predictions from MM3 energy values suggest that entropic differences and specific solvent interactions are important only to the order of several tenths of a kcal/mol. Finally, MM3 reproduces the Reeves' $\Delta 2$ stabilizing and destabilizing effect of the C-2 hydroxyl orientation on the anomeric ratio. A similar effect may help stabilize the $^1C_4$ conformers of α-altropyranose and α-idopyranose.

Acknowledgements

The authors thank Professor P.J. Garegg for several useful discussions, and Professor C. Cramer, Professor L. Dunn, Dr. G. Eggleston, and Dr. W. Franklin for pre-submission review of this work.

References

[1] J.R. Snyder and A.S. Serianni, *J. Org. Chem.*, 51 (1986) 2694–2702.
[2] D.R. Ferro, A. Provasoli, M. Ragazzi, B. Casu, G. Torri, V. Bossennec, B. Perly, P. Sinaÿ, M. Petitou, and J. Choay, *Carbohydr. Res.*, 195 (1990) 157–167.
[3] M. Rudrum and D.F. Shaw, *J. Chem. Soc.*, (1965) 52–57.
[4] R.U. Lemieux and J.D. Stevens, *Can. J. Chem.*, 44 (1966) 249–262.
[5] S.J. Angyal and V.A. Pickles, *Aust. J. Chem.*, 25 (1972) 1695–1710.
[6] M.J. Forster and B. Mulloy, *Biopolymers*, 33 (1993) 575–588.
[7] S.J. Angyal, *Angew. Chem. Int. Ed. Engl.*, 8 (1963) 157–166.
[8] P.R. Sundararajan and V.S.R. Rao, *Tetrahedron*, 24 (1968) 289–295.
[9] K.S. Vijayalakshmi and V.S.R. Rao, *Carbohydr. Res.*, 22 (1972) 413–424.
[10] M.M. Voronovitskii, A.A. Lugovskoi, and V.G. Dashevskii, *J. Struct. Chem.*, 15 (1974) 491–498.
[11] K.D. Goebel, C.E. Harvie, and D.A. Brant, *Applied Polym. Symp.*, 28 (1976) 671–691.
[12] N.V. Joshi and V.S.R. Rao, *Biopolymers*, 18 (1979) 2993–3004.
[13] K. Rasmussen, *Acta Chem. Scand. Ser. A*, 36 (1982) 323–327.
[14] J.W. Brady, *J. Am. Chem. Soc.*, 111 (1989) 5155–5165.

[15] S. Ha, J. Gao, B. Tidor, J.W. Brady, and M. Karplus, *J. Am. Chem. Soc.*, 113 (1991) 1553–1557.
[16] B.P. van Eijck, R.W.W. Hooft, and J. Kroon, *J. Phys. Chem.*, 97 (1993) 12093–12099.
[17] A. Saran and G. Govil, *Indian J. Chem.*, 9 (1971) 1095–1097.
[18] I. Tvaroška and T. Kožár, *Theor. Chim. Acta*, 70 (1986) 99–114.
[19] C.J. Cramer and D.G. Truhlar, *J. Am. Chem. Soc.*, 115 (1993) 5745–5753.
[20] P.L. Polavarapu and C.S. Ewig, *J. Comput. Chem.*, 13 (1992) 1255–1261.
[21] I. Tvaroška and J.P. Carver, *J. Chem. Res.*, (1991) 123–144.
[22] A.D. French and M.K. Dowd, *J. Mol. Struct. (Theochem)*, 186 (1993) 183–201.
[23] C. van Alsenoy, A.D. French, M. Cao., S.Q. Newton, and L. Schäfer, *J. Am. Chem. Soc.*, submitted.
[24] A.D. French and V. Tran, *Biopolymers*, 29 (1990) 1599–1611.
[25] A.D. French, N. Mouhous-Riou, and S. Pérez, *Carbohydr. Res.*, 247 (1993) 51–62.
[26] S. Cros, C. Hervé du Penhoat, S. Pérez, and A. Imberty, *Carbohydr. Res.*, 248 (1993) 81–93.
[27] H.M. Pickett and H.L. Strauss, *J. Am. Chem. Soc.*, 92 (1970) 7281–7290.
[28] H.L. Strauss, *J. Chem. Educ.*, 48 (1971) 221–223.
[29] M. Ragazzi, A. Provasoli, and D.R. Ferro, *J. Comput. Chem.*, 7 (1986) 105–112.
[30] D. Cremer and J.A. Pople, *J. Am. Chem. Soc.*, 97 (1975) 1354–1358.
[31] G.A. Jeffrey and J.H. Yates, *Carbohydr. Res.*, 74 (1979) 319–322.
[32] A.D. French and M.K. Dowd, *J. Comput. Chem.*, 15 (1994) 561–570.
[33] D.R. Ferro, A. Provasoli, and M. Ragazzi, *Carbohydr. Res.*, 228 (1992) 439–443.
[34] N.L. Allinger, Y.H. Yuh, and J.H. Lii, *J. Am. Chem. Soc.*, 111 (1989) 8551–8566.
[35] J.H. Lii and N.L. Allinger, *J. Am. Chem. Soc.*, 111 (1989) 8566–8575.
[36] N.L. Allinger, M. Rahman, and J.H. Lii, *J. Am. Chem. Soc.*, 112 (1990) 8293–8307.
[37] A.D. French, R.S. Rowland, and N.L. Allinger, *ACS Symp. Ser.*, 430 (1990) 120–140.
[38] C.A.G. Haasnoot, F.A.A.M. de Leeuw, and C. Altona, *Tetrahedron*, 36 (1980) 2783–2792.
[39] S.J. Angyal, *Adv. Carbohydr. Chem. Biochem.*, 42 (1984) 15–68.
[40] S.J. Angyal, *Adv. Carbohydr. Chem. Biochem.*, 49 (1991) 19–35.
[41] M.K. Dowd, P.J. Reilly, and A.D. French, *Biopolymers*, 34 (1994) 625–638.
[42] G.A. Jeffrey and D.-B. Huang, *Carbohydr. Res.*, 222 (1991) 47–55.
[43] A.D. French and D.P. Miller, *ACS Symp. Ser.*, 569 (1994) 235–251.
[44] M. Squillacote, R.S. Sheridan, O.L. Chapman, and F.A.L. Anet, *J. Am. Chem. Soc.*, 97 (1975) 3244–3246.
[45] F.A.L. Anet and A.J.R. Bourn, *J. Am. Chem. Soc.*, 89 (1967) 760–768.
[46] J.B. Hendrickson, *J. Am. Chem. Soc.*, 83 (1961) 4537–4547.
[47] D.A. Dixon and A. Komornicki, *J. Phys. Chem.*, 94 (1990) 5630–5636.
[48] D.M. Ferguson, I.R. Gould, W.A. Glauser, S. Schroeder, and P.A. Kollman, *J. Comput. Chem.*, 13 (1992), 525–532.
[49] G. Gatti, A.L. Segre, and C. Morandi, *J. Chem. Soc. B*, (1967) 1203–1204.
[50] P.-S. Chu and N.S. True, *J. Phys. Chem.*, 89 (1985) 2625–2630.
[51] H. Booth, K.A. Khedhair, and S.A. Readshaw, *Tetrahedron*, 43 (1987) 4699–4723.
[52] Y.-J. Zheng, S.M. Le Grand, and K.M. Merz, Jr., *J. Comput. Chem.*, 13 (1992) 772–791.
[53] J.R. Snyder, E.R. Johnston, and A.S. Serianni, *J. Am. Chem. Soc.*, 111 (1989), 2681–2687.
[54] K. Bock and H. Thøgersen, *Annu. Rep. NMR Spectrosc.*, 13 (1982) 1–57.
[55] R.E. Reeves, *Adv. Carbohydr. Chem.*, 6 (1951) 108–134.
[56] J.F. Stoddart, *Stereochemistry of Carbohydrates*, Wiley-Interscience, New York, 1971.
[57] P.E. Pfeffer, F.W. Parrish, and J. Unruh, *Carbohydr. Res.*, 84 (1980) 13–23.